N95-11127

THE USE OF VISIBLE-CHANNEL DATA FROM NOAA SATELLITES TO MEASURE TOTAL OZONE AMOUNT OVER ANTARCTICA

Robert D. Boime and Stephen G. Warren
Department of Atmospheric Sciences, AK-40
University of Washington
Seattle, Washington 98195, USA

Arnold Gruber
NOAA-NESDIS, E/RA
Washington, DC 20233, USA

ABSTRACT

Accurate, detailed maps of total ozone were not available until the launch of the Total Ozone Mapping Spectrometer (TOMS) in late 1978. However, the Scanning Radiometer (SR), an instrument on board the NOAA series satellites during the 1970s, had a visible channel that overlapped closely with the Chappuis absorption band of ozone. We are investigating whether data from the SR can be used to map Antarctic ozone prior to 1978.

The method is being developed with 1980s data from the Advanced Very High Resolution Radiometer (AVHRR), which succeeded the SR on the NOAA polar-orbiting satellites. Visible-derived total ozone maps can then be compared against maps from TOMS. Only one visible channel is available on the NOAA satellites, which precludes the use of a differential absorption technique to measure ozone. Consequently, our method works exclusively over scenes whose albedos are large and unvarying, i.e. scenes that contain ice sheets and/or uniform cloud-cover.

Initial comparisons of time series for October-December 1987 at locations in East Antarctica show that the visible absorption by ozone is measurable and that the technique may be usable for the 1970s, but with much less accuracy than TOMS. This initial test assumes that clouds, snow, and ice all reflect the same percentage of visible light towards the satellite, regardless of satellite position or environmental conditions. This assumption is our greatest source of error. To improve the accuracy of ozone retrievals, realistic anisotropic reflectance factors are needed, which are strongly influenced by cloud and snow surface features.

1. INTRODUCTION

The Antarctic ozone hole appears to have developed rapidly beginning about the same time that the Total Ozone Mapping Spectrometer (TOMS) was launched in late 1978. Evidence for ozone changes prior to that time is limited to ground-based measurements from a few Antarctic stations and unreliable satellite data, which suggest a slow decrease during the 1970s. The ozone amounts mapped by TOMS show large spatial and temporal variation on scales of a few hundred kilometers and a few days (Yung et al., 1990). A few isolated stations therefore cannot adequately represent the entire continent, so it would be useful to find a method to map the spatial variation of total ozone over Antarctica prior to 1978.

Radiometer data from NOAA polar-orbiting satellites may contain information about the early evolution of the ozone hole above Antarctica. These instruments have a visible channel that is centered on a weak absorption band of ozone at 600-nm wavelength (figure 1), where the other constituents in the Antarctic atmosphere and surface, including clouds and snow, are non-absorptive. The visible-channel data have been gridded and archived by NOAA beginning 1974, and the early measurements do show decreasing absorption as solar elevation increases (figure 2). This dependence is apparently due to the shorter slant path through the ozone layer with increasing solar elevation, indicating that

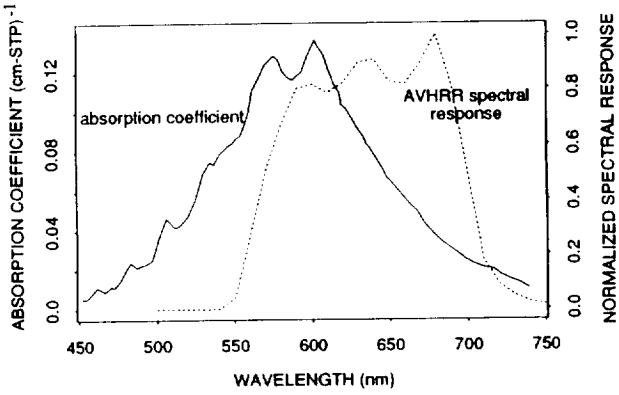

Figure 1. The Chappuis absorption band of ozone and the spectral response of the AVHRR visible channel on the NOAA-9 spacecraft. Maximum overlap occurs near 600 nm. The absorption coefficients for the Chappuis band are taken from Vigroux (1953) and the channel response values are from Rossow el al. (1985).

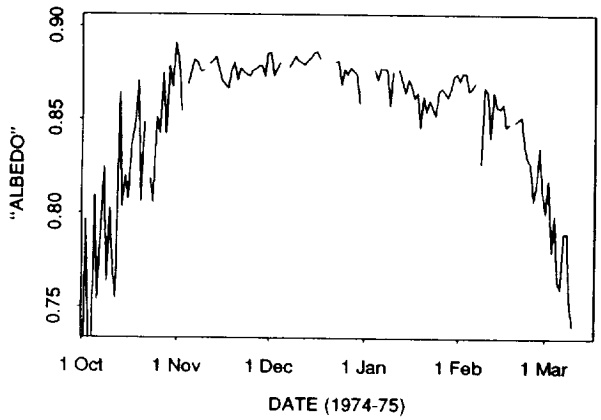

Figure 2. Daily values of "albedo" (assuming isotropic reflectance) from September 1974 to February 1975 at South Pole. The albedo rises from 0.78 in October to 0.88 in December, just what one would expect for a normal unchanging column ozone amount of 300 DU (figure 2 of Wiscombe and Warren, 1980). The lower albedo in October is due to the longer slant path through the ozone at low solar elevation angles. The data were taken by the Scanning Radiometer (SR), the predecessor to the Advanced Very High Resolution Radiometer (AVHRR).

visible absorption by ozone is indeed significant so that variations in ozone amount should be detectable.

In this initial evaluation of the method's feasibility, we apply a simple analysis to satellite data taken during October-December 1987 by the NOAA-9 AVHRR. The calculation incorporates only absorption by ozone and reflection by the clouds and snow below, ignoring Rayleigh scattering. Use of the 1980s data allows a comparison between our retrieved ozone amounts with those from TOMS.

The AVHRR has a spatial resolution of 1.1 km and an intensity count resolution or 0.1% (ten bits). However, in order to obtain large spatial and temporal coverage, it is convenient in this initial test to use the "level B3" data of the International Satellite Cloud Climatology Project (ISCCP; Rossow et al., 1987). For the B3 archive, the original 1.1-km data are sampled to 30-km resolution, and the 10-bit counts are truncated to 8 bits.

2. METHOD

The simplest possible method for deriving total ozone amount from a visible-channel measurement uses a calculation of two-way transmittance:

$$I = \frac{Q_0 A_s \chi}{\pi} \cos\theta_0 \exp\{-0.0796u[x(\theta_0) + \sec\theta]\}. \quad (1)$$

Q_0 is a fraction of the solar constant: the integral of the incident solar spectral irradiance at the top of the atmosphere normal to the solar beam, weighted by the channel sensitivity function (figure 1). Radiation from the sun passes through the ozone layer of thickness u (cm-STP) through pathlength x, a function of solar zenith angle θ_0. Large solar zenith angles are typical in Antarctic latitudes, so the effect of Earth's curvature must be taken into account when calculating pathlength. The function $x(\theta_0)$ is given by Rozenberg (1966):

$$x = \frac{1}{\cos\theta_0 + 0.025\exp(-11\cos\theta_0)}. \quad (2)$$

Note that when $\theta_0 < 70^\circ$, $x \approx \sec\theta_0$.

Once the solar beam has passed through the ozone layer, it encounters everything beneath the layer, including clouds, snow and ice. The sub-ozone layer has albedo A_s and anisotropic reflectance factor χ: a function of θ_0, θ, and ϕ, where θ is the satellite zenith angle and ϕ is the relative azimuth angle between sun and satellite. χ is defined such that its average value over the upward hemisphere is 1.0. The reflected radiation passes through the ozone layer again at angle θ to reach the satellite. Given a measurement of intensity I by the radiometer, equation (1) is solved for u. The units are W m^{-2} sr^{-1} for intensity I, W m^{-2} for irradiance Q_0, and sr for π.

The ozone absorption coefficient in (1) is 0.0796 $(cm\text{-}STP)^{-1}$, which is an average of the Chappuis band (figure 1), weighted by the NOAA-9 AVHRR visible channel-function (also shown in figure 1). This absorption coefficient will differ somewhat for different satellites, because of differences in their channel-functions.

Over dark surfaces, variations in u or θ_0 have little effect on the planetary albedo at 600 nm because most of the radiation not absorbed by ozone is absorbed by the underlying surface. Uniform snow surfaces, however, have very high albedo at 600 nm, about 0.97 (Warren et al., 1986), which is the value we use for A_s. The near-infrared albedo is much lower, giving the familiar value for spectrally-averaged solar albedo of 80-85% for Antarctic snow. Because the visible surface albedo is already so high, clouds do not significantly change the albedo at the top of the atmosphere.

Equation (1) neglects scattering by the atmosphere above the ozone layer. Polar stratospheric clouds can exist within and partially above the ozone layer, but their typical optical depth is about 0.01 (Kinne and Toon, 1990). The optical depth is somewhat greater over mountainous areas, but our method has other difficulties in those regions as well. Rayleigh scattering is weak at 600 nm, and only a few percent of the atmospheric mass is above the ozone, so it is ignored as well. The effect of Rayleigh scattering *below* the ozone layer will most likely cause the anisotropic reflectance factor χ for the sub-ozone scene to be slightly more isotropic than that of the snow or cloud surface. These are effects that can be incorporated in a remote-sensing method for ozone retrieval, but we think they are all far less important than the inclusion of a realistic χ for clouds and snow, discussed below.

Due to the limited spatial and intensity resolution in the ISCCP-B3 data used for this initial test, the uncertainty in θ_0, θ and I result in an inherent uncertainty of 60 Dobson units (DU) for each derived u value. However, the satellite passes above the polar regions several times per day and the pixel size is on the order of tens of kilometers while ozone varies over a few hundred kilometers. Approximately 100 derived u values can, therefore, be binned and averaged into a single value on any given day without loss of map resolution. Ran-

dom error due to finite data resolution is then reduced to 6 DU per mapped u value.

3. REFLECTION FROM CLOUDS AND SNOW

The anisotropic reflectance factor χ of the sub-ozone layer is by far the most uncertain quantity in (1). The retrieved ozone amount is sensitive to χ because the visible absorption by ozone is so weak. Typically, the derived total column ozone increases by 50-100 DU with a few-percent decrease in the assumed value of χ in the satellite's direction. (The direction of the satellite with respect to the pixel being scanned is defined by θ and ϕ.) To evaluate the importance of knowing χ, we are as a first step seeing how well (or how poorly) ozone amounts can be calculated by assigning $\chi = 0.9$ in the satellite's direction, independent of angle, location or season. This is a good approximation given typical values of θ_0, θ and ϕ encountered in the data used for this analysis. However, because u is highly sensitive to χ, in future analyses we will require a detailed knowledge of the anisotropic reflectance of the sub-ozone scene.

Small longitudinal dunes called sastrugi cover nearly the entire Antarctic ice sheet. They cause χ to depend not only on θ_0, θ, and ϕ, but also on the azimuth of the sun relative to the prevailing wind direction. Because the dunes align themselves parallel to the wind, the prevailing wind direction is called the sastrugi axis. A flat snow surface has a forward-peaked χ like most natural surfaces. This normal forward-scattering pattern also results from a sastrugi field when the solar beam is parallel to the sastrugi axis, but a backward peak in χ can result when the solar beam is perpendicular to the sastrugi axis. If the sun is low enough, the sastrugi will even cast shadows, further enhancing the backward peak. The sastrugi vary in orientation and height across Antarctica. Their predominant orientations are fairly well established and have been mapped by Parish and Bromwich (1987).

Although clouds do not change the top-of-atmosphere albedo much, they can change χ dramatically. Clouds tend to scatter radiation in the forward direction. Putting a cloud over a flat snow surface would change χ very little since flat snow tends to be forward-scattering also. However, as discussed above, sastrugi can strongly scatter radiation backwards. Thus cloud cover is expected to alter χ more in October (when the sastrugi are well-developed) than in January (when the surface is relatively flat). It will therefore be important in future work to find a way either to detect clouds or to remove their influence. This may possibly be done by making use of the fact that cloud cover has a higher frequency of variability in time than total ozone.

4. AVHRR-DERIVED OZONE AMOUNTS, COMPARED TO TOMS

Figure 3 shows time series of total ozone derived from AVHRR and TOMS at three locations over East Antarctica. At site 3a, there is more noise in the AVHRR-derived time series than in the TOMS-derived series, and the values in October are too low while those in late December are too

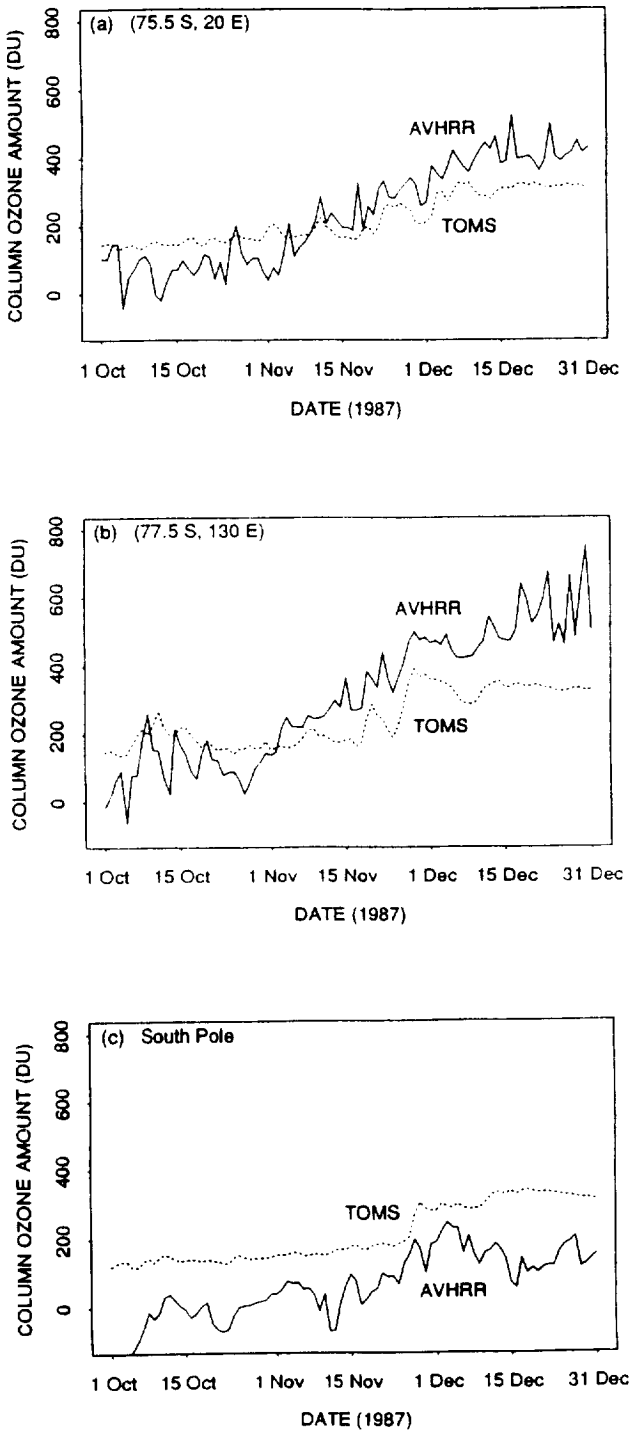

Figure 3. Time series from 1 October to 31 December 1987 of total ozone derived from the visible channel of AVHRR and from TOMS at (a) 75.5 S, 20 E, (b) 77.5 S, 130 E, and (c) South Pole.

high. However, the two series follow a similar pattern: column ozone stays relatively constant until November and then begins a gradual ascent (when the ozone hole begins to disappear). The daily values are best correlated in late November and early December. The correlation coefficient between the two 3-month series is 0.90.

Site 3b is located approximately 2400 km from site 3a on the other side of East Antarctica. Here again, October and December values differ and the visible-derived series is noisier; however, the two series follow a similar trend. They show an initial rise in column ozone in early October, a small decline later in the month and then a strong rise through November. The correlation coefficient between the two series in this case is 0.88. Similar to the events at site 3a, the series at 3b are best correlated in late November and early December.

The AVHRR-derived time series are noisier than the TOMS-derived series partially because of cloud interference in October when sastrugi are higher and of decreased sensitivity to ozone in December when the path length of the solar beam through the layer is shortest. The separation of the series in October and December at the two sites illustrates the failure of our initial assumption that the sub-ozone anisotropic reflectance is constant. In October, there is preferential scattering by sastrugi towards the satellite, which forces equation (1) to calculate a thinner layer of ozone to account for the extra radiation the instrument is seeing. Conversely, in December, there is preferential scattering away from the satellite by the flat snow surface which causes equation (1) to infer a thick ozone layer. The anisotropic reflectance factor χ will also depend on the solar zenith angle θ_0 which is highest in October and lowest in December.

Finally, site 3c is South Pole. There is considerable spatial variance in u near the pole which has been averaged out in Figure 3c: all 30-km pixels from the zone 85 S to 90 S were averaged together for this figure. This zone has 16 times the area used at the two other sites to calculate each data point in the time series. Once again, the AVHRR derived series is noisier and there is systematic downward offset, even exhibiting negative values of total ozone in October and November. A negative value implies that so much more radiation is reaching the satellite than would be expected under the constant-χ assumption, that the exponent in equation (1) becomes positive to explain it. However, the two series are similar in that they show the jump in total ozone around 30 November, marking the recovery from the 1987 ozone hole at South Pole. The correlation coefficient in this case is 0.79.

5. CONCLUSION

By modeling the transfer of visible radiation through the Antarctic atmosphere, we have attempted to obtain column ozone from the visible channel of the AVHRR. Results of the initial investigation show promise in this technique, especially considering the simplicity of the analysis method and the coarse resolution of the data. The fact that the visible-derived time series of total ozone correlate with the UV-derived values in figure 3 suggest that it would be worthwhile to continue investigation of the visible data by improving the method of analysis.

In future work the description of surface-atmosphere reflectance can be improved by employing cloud observations, sastrugi models and statistical analysis. Rayleigh scattering by the sub-ozone atmosphere can be readily incorporated. Estimates of anisotropic reflectance factors will be obtained from both satellite data and surface data: (a) We will determine the values of χ that give us the correct (TOMS) values of total ozone for October-December 1987 when put into equation 1. (b) We are now measuring χ for natural sastrugi surfaces from a tower at the South Pole Station at all values of solar azimuth angle relative to the sastrugi axis.

If the method appears useful after these improvements have been made, the technique can be applied to Scanning Radiometer data from the 1970s.

REFERENCES

Kinne, S., and O. B. Toon, 1990: Radiative effects of polar stratospheric clouds. Geophys. Res. Lett., 17, 373-376.

Parish, T.R., and D.H. Bromwich, 1987: The surface windfield over the Antarctic ice sheets. Nature, 328, 51-54.

Rossow, W. B., E. Kinsella, A. Wolf, and L. Gardner, 1985: International Satellite Cloud Climatology Project (ISCCP), description of reduced resolution radiance data. WMO/TD No. 58.

Rozenberg, G. V., 1966: Twilight; A Study In Atmospheric Optics. Plenum Press, New York, 358 pp.

Vigroux, E., 1953: Contribution à l'étude expérimentale de l'absorption de l'ozone. Annales de Physique 8, 709-762.

Warren, S. G., T.C. Grenfell, and P.C. Mullen, 1986: Optical properties of Antarctic snow. Antarctic J. U. S., 21, 247-248.

Wiscombe, W.J., and S. G. Warren, 1980: Solar and infrared radiation calculations for the Antarctic Plateau using a spectrally-detailed snow reflectance model. International Radiation Symposium Volume of Extended Abstracts, Colorado State Univ., 380-382.

Yung, Y.L., M. Allen, D. Crisp, R.W. Zurek, and S.P. Sander, 1990: Spatial variation of ozone depletion rates in the springtime Antarctic polar vortex. Science, 248, 721-724.